Two-soliton interaction in the vicinity of a defect inside a fiber Bragg grating and its application for obtaining an all-optical memory

Yuval P. Shapira* and Moshe Horowitz

Department of Electrical Engineering, Technion—Israel Institute of Technology, Haifa 32000, Israel
**Corresponding author: yuvalsh@tx.technion.ac.il*

Received October 16, 2007; revised December 19, 2007; accepted December 21, 2007;
posted February 27, 2008 (Doc. ID 88528); published March 26, 2008

We study the interaction between two Bragg solitons in the vicinity of a defect inside a fiber Bragg grating. A soliton that is trapped in the defect can be released by launching a second soliton. The effect can be used to obtain an all-optical memory that is not strongly sensitive to the phase and the timing arrival of the solitons. © 2008 Optical Society of America

OCIS codes: 050.2770, 060.4370, 060.5530, 060.2340, 230.1150.

Bragg solitons are solitary waves that can propagate in a fiber Bragg grating (FBG) with a velocity that can be significantly lower than the speed of light in the fiber [1,2]. It has been shown that two counterpropagating Bragg solitons can merge into a single standing localized pulse [3,4]. The method is sensitive to soliton phases. Solitons can also be localized by introducing a defect into the grating [5,6]. This latter method is not sensitive to the soliton phase, and it can also be applied to low-intensity solitons. In this Letter we show that a control soliton can be used to release a soliton that is trapped in a defect inside a FBG. The trapped soliton is released regardless of both the phase and the delay of the control soliton, as was verified numerically for a large set of parameters. We give a physical explanation of the interaction by considering the spatial asymmetry induced in the local grating parameters due to the Kerr effect. The novel interaction can be used to obtain a 1 bit all-optical memory. We note that an all-optical memory has been previously theoretically demonstrated by using optical solitons in a resonant photonic crystal [7]. However, the device operation reported in [7] was strongly sensitive to the arrival time of the control soliton, unlike in the device reported here.

Wave propagation in nonuniform FBGs with Kerr nonlinearity is described by nonlinear coupled mode equations:

$$\pm i\partial_z u_\pm + iV_g^{-1}\partial_t u_\pm + \kappa_L(z)u_\mp + \Gamma(|u_\pm|^2 + 2|u_\mp|^2)u_\pm + \sigma_L(z)u_\pm = 0, \quad (1)$$

where $u_\pm$ are the slowly varying amplitudes of the forward (+) and the backward (−) propagating waves, Γ is the nonlinear coefficient, $V_g = c/n_{\text{eff}}$ is the group velocity in the absence of the grating, n_{eff} is the effective refractive index, $\kappa_L(z)$ is the grating strength, and $\sigma_L(z)$ is the chirp parameter [8].

We demonstrate the soliton interaction in the vicinity of a defect by using a grating with the chirp function shown in Fig. 1. The defect used in this work is obtained by adding a local perturbation to the chirp parameter in the center of region II of the grating, at $z=0$. The defect is given by $\sigma_{\text{def}}(z) = 5.75[\cos(2\pi z/\Delta z)+1]\ \text{m}^{-1}$ with $\Delta z = 0.8$ mm. The defect length is significantly smaller than the spatial width of the solitons propagating in the grating. The defect length is, however, 3 orders of magnitude larger than the grating period, and hence the field's propagation around the defect can be accurately analyzed by using Eq. (1). Besides adding the defect, the grating is similar to that used for obtaining an AND gate [9]. Region II of the grating is used to trap the soliton, while regions I and III are used to accelerate the soliton after its release.

The lengths of the three grating regions are $L_1 = L_3 = 5.14$ cm and $L_2 = 0.78$ cm, and hence the total grating length is 11.06 cm. The grating parameters are $\kappa = 9000\ \text{m}^{-1}$, $n_{\text{eff}} = 1.45$, and $\sigma_L(z)$, with $\sigma_L(z) - \sigma_{\text{def}}(z)$ being a piecewise linear function of z with a slope of $888.6\ \text{m}^{-2}$ in regions I, $-888.6\ \text{m}^{-2}$ in region III, and zero in region II. The nonlinear coefficient is equal to $\Gamma = 5\ \text{km}^{-1}\,\text{W}^{-1}$. The input solitons have a spatial full width at half-maximum (FWHM) of 0.39 cm, an energy of 64.014 nJ, and a frequency offset of 297.478 GHz with respect to the local Bragg frequency at the beginning of region I.

We have simulated the wave propagation in the grating by using the split-step method [10]. The results of the simulation are shown in Fig. 2. At $t=0$ a soliton with initial phase $\phi = 5.9$ rad was launched at $z = -6.7$ cm. The soliton was trapped inside region II, and it oscillated around the defect with a spatial amplitude that decayed over time, as is shown in Fig. 2(a). At $t = 20$ ns the spatial amplitude of the oscillation was about 0.5 mm, and the soliton lost about 10% of its initial energy. At $t = 15.9$ ns a control soli-

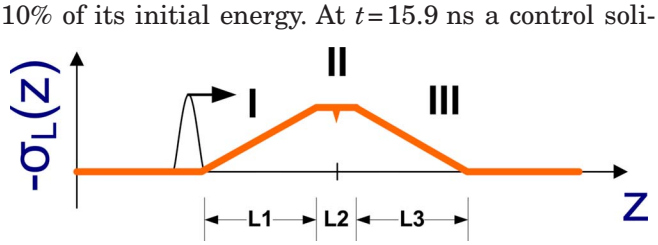

Fig. 1. (Color online) Schematic structure of the grating chirp parameter used to obtain the optical memory.

0146-9592/08/070675-3/$15.00

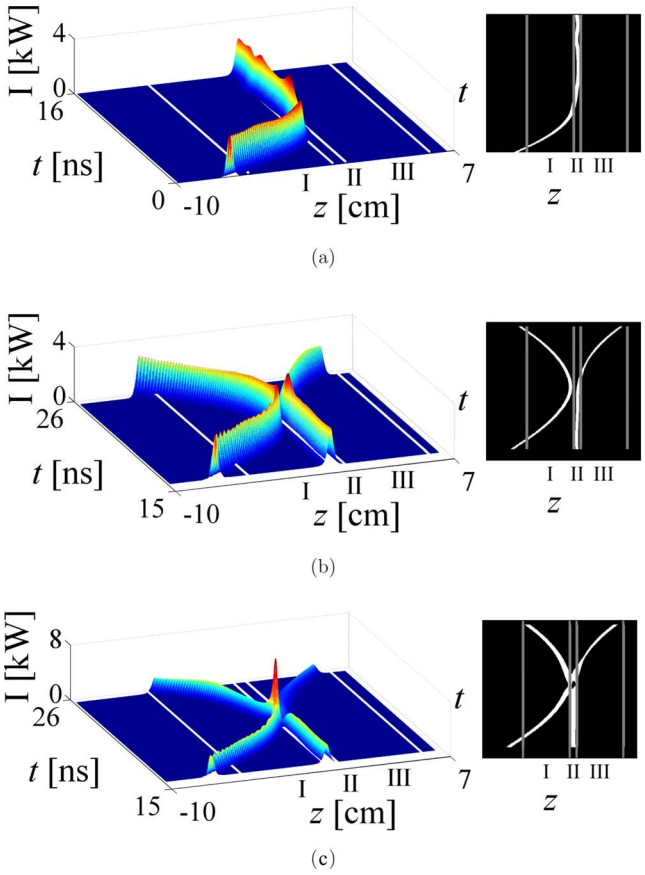

Fig. 2. (Color online) Simulation results showing the intensity I of the waves propagating in the grating in the case when (a) a single soliton is trapped, and in cases when a trapped soliton is released by a control soliton with an initial phase (b) $\phi=12\pi/10$ and (c) $\phi=2\pi/10$.

ton was launched at $z=-7.1$ cm with an initial phase $\phi=12\pi/10$ rad [Fig. 2(b)] and another with an initial phase $\phi=2\pi/10$ rad [Fig. 2(c)]. In both cases, the interaction between the two solitons caused the release of the trapped soliton. In the case shown in Fig. 2(b), the trapped soliton moved toward the $+z$ direction and the control soliton was backreflected. In the case shown in Fig. 2(c), the two solitons spatially overlapped. Our physical interpretation given below indicates that in this case the trapped soliton was released and propagated toward the $-z$ direction while the control soliton was transmitted.

We have simulated the release of the trapped soliton for 20 different initial phases of the control soliton. For all the initial phases that were checked, the trapped soliton was released, and after the interaction ended two counterpropagating pulses exited the grating. The energies of the backward and the forward propagating pulses after the interaction are shown in Fig. 3. Although the energies of the two counterpropagating pulses change as a function of the initial phase of the control soliton, the trapped pulse was released for all the initial phases that were checked. Since the trapped soliton oscillates around the defect with a periodicity of about 6.4 ns, we have also verified that the trapped soliton was released at nine different launching times of the control soliton, equally distributed between $t=16$ ns and $t=23$ ns.

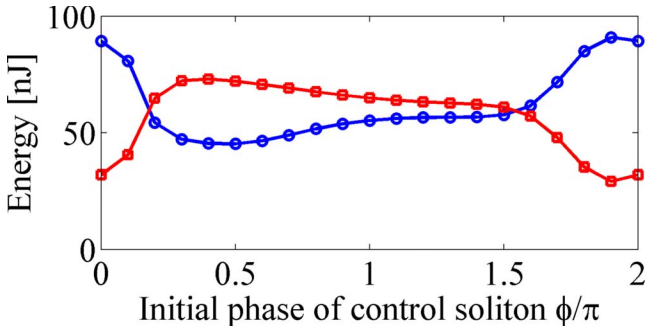

Fig. 3. (Color online) Energy of the forward (circles) and the backward (squares) propagating solitons after the trapped soliton was released, as function of the control soliton phase.

For each launching time, ten different phases of the control soliton were simulated.

We note that in a practical grating the lifetime of the trapped soliton is limited owing to grating loss [11]. However, the loss in FBGs can be reduced by using deuterium-loaded fibers, by optimizing the writing procedure, and by adding a small gain that compensates for the loss. Assuming a loss of 0.1 dB/m, the energy of the input wave decays to 50% of its initial value after about 0.15 μs. This time duration is about ten times longer than the time needed to release the trapped soliton. Therefore, we have neglected the absorbtion effect in our simulations. The loss can be also overcome by utilizing a refresh procedure as used in electronic devices.

To obtain a physical insight into the soliton interaction, we have studied the local, time-varying changes in the grating structure caused by the Kerr effect. We rewrite Eq. (1):

$$\pm i\partial_z u_\pm + iV_g^{-1}\partial_t u_\pm + \hat{q}_\pm(z;t)u_\mp + \hat{\sigma}(z;t)u_\pm = 0, \quad (2)$$

where $\hat{\sigma}(z;t)=\sigma_L(z)+\sigma_{NL}(z;t)$, $\sigma_{NL}(z;t)=\Gamma(|u_+|^2+|u_-|^2)$ and $\hat{q}_\pm(z;t)=\kappa_L(z)+q_{NL\pm}(z;t)$, $q_{NL\pm}(z;t)=\Gamma u_\mp^* u_\pm$. Equation (2) describes wave propagation in a linear nonuniform grating that varies in time, with parameters $\hat{\sigma}(z;t)$ and $\hat{q}_\pm(z;t)$. We define $\hat{q}(z;t)$ and $\theta(z;t)$ as the amplitude and the phase of $\hat{q}_\pm(z;t)$: $\hat{q}_\pm(z;t)=\hat{q}(z;t)\exp(\pm j\theta(z;t))$. The local Bragg frequency shift with respect to the local Bragg frequency at the beginning of region I is given by $\Delta\Omega_B(z;t)=\Delta\Omega_L(z)+\Delta\Omega_{NL}(z;t)$, where $\Delta\Omega_L(z)=-V_g\sigma_L(z)$ is the frequency shift caused by the chirp of the grating and the defect and $\Delta\Omega_{NL}(z;t)=V_g(\frac{1}{2}\partial_z\theta(z;t)-\sigma_{NL}(z;t))$ is the frequency shift caused by nonlinearity. The local grating strength is given by $\kappa(z;t)=\kappa_L(z)+\Delta\kappa_{NL}(z;t)$, where $\Delta\kappa_{NL}(z;t)=\hat{q}(z;t)-\kappa_L(z)$ is the change in the local grating strength caused by nonlinearity.

Figure 4 shows the change in the local Bragg frequency of the grating, $\Delta\Omega_{NL}$, for two different initial phases of the control soliton as used in Figs. 2(b) and 2(c). The grating parameters are shown at the beginning of the interaction when the distance between the solitons peaks was approximately 1.17 and 0.96 cm. In each plot we compare the grating parameters in the case when the soliton interaction exists

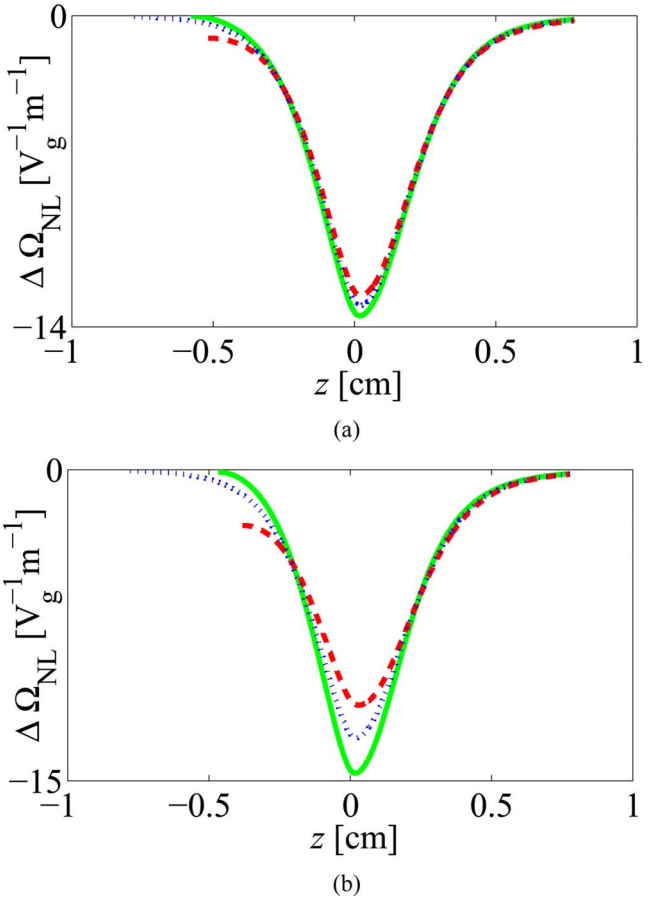

Fig. 4. (Color online) Local nonlinear Bragg frequency shift, $\Delta\Omega_{\mathrm{NL}}(z;t)$, in the beginning of the interaction at (a) $t=19.7$ ns and (b) $t=20.1$ ns, calculated for the cases when the control soliton was launched with an initial phase of $\phi=12\pi/10$ (solid curve) and of $\phi=2\pi/10$ (dashed curve) and for the case when the control soliton was not launched (dotted curve).

and in the case when the control soliton is not launched. The interaction between the solitons causes a change in the grating parameters. Since the spatial FWHM of the soliton is about $35\kappa_{\mathrm{L}}^{-1}$, and since a uniform grating section with a length of $3\kappa_{\mathrm{L}}^{-1}$ reflects about 99% of the power of an incident wave located inside the bandgap of this section, there is a physical meaning in referring to changes in the local bandgap in the grating regions where the soliton power is low and the waves are backreflected. At a given time, the local reflectivity, i.e., the reflectivity from a short section of the time-varying grating, decreases as the nonlinear Bragg frequency shift $\Delta\Omega_{\mathrm{NL}}$ decreases and as the nonlinear grating strength $\Delta\kappa_{\mathrm{NL}}$ decreases, since the central soliton frequency is located around the upper frequency edge of the grating bandgap [1]. In the case shown in Fig. 2, the soliton velocity in the interaction region is very small, and hence $|u_+(z;t)| \simeq |u_-(z;t)|$. Therefore, $\Delta\kappa_{\mathrm{NL}}(z;t) \simeq 0.5\Delta\Omega_{\mathrm{NL}}(z;t)$, and both $\Delta\kappa_{\mathrm{NL}}$ and $\Delta\Omega_{\mathrm{NL}}$ have a similar effect on the local grating reflectivity.

The interaction between the solitons causes a spatial asymmetry in the grating parameters with respect to the center of the trapped soliton. The asymmetry was maintained during all of the beginning of the interaction as indicated by Fig. 4. In the case $\phi=12\pi/10$, the interaction increases the local reflectivity in the region where the left tail of the trapped soliton is located because of destructive interference between the two soliton fields in that region. Therefore, the soliton is pushed toward the $+z$ direction, whereas the control soliton is pushed toward the $-z$ direction. Owing to the grating chirp in region III, the soliton accelerates and is released toward the $+z$ direction. In the case $\phi=2\pi/10$ the interference in the left tail region of the trapped soliton is constructive. As a result, the local reflectivity in that region is decreased, the trapped soliton is pushed toward the $-z$ direction, and the control soliton is pushed toward the $+z$ direction. Similar asymmetries in the grating profile with respect to the trapped soliton center were observed for all the different phases that were used to calculate Fig. 3. We note that at a certain time and for a specific phase of the control soliton, the interference does not cause an asymmetry in the grating parameters. However, because of the relative movement of the two solitons, this condition is not maintained, and an asymmetry in the grating profile is eventually obtained. Hence, the trapped soliton can be released regardless of the initial phase of the control soliton.

In conclusion, we have demonstrated an optical memory based on an all-optical trapping and releasing of an optical soliton, using a novel soliton interaction in the vicinity of a defect inside a fiber Bragg grating. The release of the trapped soliton did not depend on the phase and the delay of the control soliton, as was verified numerically for a large set of parameters. We have given a physical explanation of the results based on calculating the local change in the grating parameters due to nonlinear interaction. The nonlinear interaction causes an asymmetry in the grating parameters that is responsible for the release of the trapped soliton.

This work was supported by the Israel Science Foundation (ISF) of the Israeli Academy of Sciences.

References

1. C. M. de Sterke and J. E. Sipe, in *Progress in Optics XXXIII*, E. Wolf ed. (Elsevier, 1994), pp. 203–260.
2. J. T. Mok, C. M. de Sterke, I. C. M. Littler, and B. J. Eggleton, Nat. Phys. **2**, 775 (2006).
3. W. C. K. Mak, B. A. Malomed, and P. L. Chu, Phys. Rev. E **68**, 026609 (2003).
4. D. R. Neill and J. Atai, Phys. Lett. A **353**, 416 (2006).
5. R. H. Goodman, R. E. Slusher, and M. I. Weinstein, J. Opt. Soc. Am. B **19**, 1635 (2002).
6. W. C. K. Mak, B. A. Malomed, and P. L. Chu, J. Opt. Soc. Am. B **20**, 725 (2003).
7. I. V. Mel'nikov and J. S. Aitchison, Appl. Phys. Lett. **87**, 201111 (2005).
8. C. M. de Sterke, J. Lightwave Technol. **17**, 2405 (1999).
9. Y. P. Shapira and M. Horowitz, Opt. Lett. **32**, 1211 (2007).
10. A. Rosenthal and M. Horowitz, Opt. Lett. **31**, 1334 (2006).
11. P. Niay, M. Douay, P. Bernage, W. X. Xie, B. Leconte, D. Ramecourt, E. Delevaque, J. F. Bayon, H. Poignant, and B. Poumellec, Opt. Mater. **11**, 115 (1999).